Infection by tubercular mycobacteria is spread by nonlytic ejection from their amoeba hosts

Hagedorn, Monica; Rohde, Kyle H; Russell, David G; Soldati, Thierry

Science
AAAS

Infection by Tubercular Mycobacteria Is Spread by Nonlytic Ejection from Their Amoeba Hosts

Monica Hagedorn, *et al.*

Science **323**, 1729 (2009);
DOI: 10.1126/science.1169381

why the initial CD8 T cell response should result in such divergent outcomes.

We determined by ISTH that strain LCMV-Armstrong is cleared because the number of immune effectors rapidly exceeds the number of infected cells. LCMV–clone 13, on the other hand, immediately infects larger numbers of macrophages (*18*) and fibroreticular cells (FRCs) (*20*) than does LCMV-Armstrong, thereby exceeding the capacity of the initial immune response to reduce the basic reproductive rate below 1 and thereby contain infection.

The divergent outcome and larger number of cells infected by LCMV–clone 13 in the spleen are illustrated in Fig. 3, which tracks LCMV RNA$^+$ cells and LCMV-antigen$^+$ FRCs (*13*) in the spleen from 1 to 8 dpi for the respective strains. As previously described, both strains of LCMV infect splenic marginal zone macrophages and FRCs in the white pulp, but LCMV–clone 13 infects larger numbers of both cell types (*18*, *20*). This difference, particularly the infection of FRCs, is already evident at 1 dpi, as judged by the diffuse ISH signal emanating from LCMV RNA$^+$ cells in the white pulp. LCMV–clone 13 infection of both cell types is sustained at high levels at 3, 5, and 8 dpi, whereas the numbers of LCMV-Armstrong–infected cells are barely detectable by 8 dpi.

The different infection outcomes produced by these two strains of LCMV cannot be explained by differences in the immune response seen in FACS analysis, but can be explained by ISTH, which provides the critical relevant measure of relative rates of increase in effectors and targets. By FACS analysis, the rapidly expanding populations of virus-specific tetramer$^+$ T cells were comparable for both strains from 3 to 8 dpi (Fig. 4A). However, E:T ratios determined by ISH reflect the increase of infected cells (relative to LCMV-GP and NP-tetramer$^+$ cells) in LCMV–clone 13 infection versus LCMV-Armstrong infection (Fig. 4B). Because of the faster increase of infected cells relative to LCMV-tetramer$^+$ cells, the E:T ratio for LCMV–clone 13 never approached 1. By contrast, the E:T ratio for LCMV-Armstrong was already ~4 at 3 dpi, higher than the ratio for LCMV–clone 13 at 3 dpi by a factor of 20.

Together, the ISTH analyses of SIV and LCMV infection tell us that location, timing, and numbers of effectors and targets all count in determining outcome. We have speculated elsewhere (*5*) that if the "too little, too late" response to SIV infection (*7*) had occurred earlier, when there were only small founder populations of infected cells confined to the portal of entry, vaginal transmission and systemic infection might be prevented with relatively few effector cells. Thus, in SIV (and, by extension, HIV-1) infections, a vaccine that elicited an immune response at the portal of entry "enough and soon enough" could prevent vaginal transmission.

References and Notes

1. P. C. Doherty, *Science* **280**, 227 (1998).
2. R. A. Koup *et al.*, *J. Virol.* **68**, 4650 (1994).
3. M. J. Kuroda *et al.*, *J. Immunol.* **162**, 5127 (1999).
4. M. P. Davenport, R. M. Ribeiro, A. S. Perelson, *J. Virol.* **78**, 10096 (2004).
5. A. T. Haase, *Nat. Rev. Immunol.* **5**, 783 (2005).
6. M. Pope, A. T. Haase, *Nat. Med.* **9**, 847 (2003).
7. M. R. Reynolds *et al.*, *J. Virol.* **79**, 9228 (2005).
8. Q. Li *et al.*, *Nature* **434**, 1148 (2005).
9. J. J. Mattapallil *et al.*, *Nature* **434**, 1093 (2005).
10. R. S. Veazey *et al.*, *Science* **280**, 427 (1998).
11. R. Ahmed, A. Salmi, L. D. Butler, J. M. Chiller, M. B. Oldstone, *J. Exp. Med.* **160**, 521 (1984).
12. E. J. Wherry, J. N. Blattman, K. Murali-Krishna, R. van der Most, R. Ahmed, *J. Virol.* **77**, 4911 (2003).
13. See supporting material on *Science* Online.
14. P. J. Skinner, M. A. Daniels, C. S. Schmidt, S. C. Jameson, A. T. Haase, *J. Immunol.* **165**, 613 (2000).
15. C. J. Miller *et al.*, *J. Virol.* **79**, 9217 (2005).
16. B. R. Mothe *et al.*, *J. Virol.* **76**, 875 (2002).
17. D. L. Barber *et al.*, *Nature* **439**, 682 (2006).
18. M. Matloubian, S. R. Kolhekar, T. Somasundaram, R. Ahmed, *J. Virol.* **67**, 7340 (1993).
19. M. Matloubian, T. Somasundaram, S. R. Kolhekar, R. Selvakumar, R. Ahmed, *J. Exp. Med.* **172**, 1043 (1990).
20. S. N. Mueller *et al.*, *Proc. Natl. Acad. Sci. U.S.A.* **104**, 15430 (2007).

21. We thank the Immunology Core Laboratory and Primate Services Unit of the California National Primate Research Center (CNPRC); D. Lu, T. Rourke, R. Dizon, and B. Vang for technical assistance; J. Sedgewick for assistance in setting up the confocal microscope to capture images of silver grains; D. Masopust for helpful discussion; and C. O'Neill and T. Leonard for help in preparing the manuscript and figures. Supported in part by NIH research grants AI48484 (A.T.H.), AI20048 (R.A.), and AI066314 (C.J.M.); National Center for Research Resources grant RR00169 (CNPRC, University of California, Davis); and a gift from the James B. Pendleton Charitable Trust (C.J.M.).

Supporting Online Material

www.sciencemag.org/cgi/content/full/323/5922/1726/DC1
Materials and Methods
Fig. S1
References

18 November 2008; accepted 9 February 2009
10.1126/science.1168676

Infection by Tubercular Mycobacteria Is Spread by Nonlytic Ejection from Their Amoeba Hosts

Monica Hagedorn,[1] Kyle H. Rohde,[2] David G. Russell,[2] Thierry Soldati[1]*

To generate efficient vaccines and cures for *Mycobacterium tuberculosis*, we need a far better understanding of its modes of infection, persistence, and spreading. Host cell entry and the establishment of a replication niche are well understood, but little is known about how tubercular mycobacteria exit host cells and disseminate the infection. Using the social amoeba *Dictyostelium* as a genetically tractable host for pathogenic mycobacteria, we discovered that *M. tuberculosis* and *M. marinum*, but not *M. avium*, are ejected from the cell through an actin-based structure, the ejectosome. This conserved nonlytic spreading mechanism requires a cytoskeleton regulator from the host and an intact mycobacterial ESX-1 secretion system. This insight offers new directions for research into the spreading of tubercular mycobacteria infections in mammalian cells.

Intracellular bacterial pathogens have evolved strategies to exploit host cell resources and replicate inside a variety of cell types, staying out of reach of the host's immune system. The concept is emerging that pathogenic bacteria evolved from environmental species by adapting to an intracellular lifestyle within free-living bacteria-eating protozoans. Consequently, cellular defense mechanisms that are active in animal immune phagocytes may have originated in amoebas (*1*, *2*). For example, during differentiation of the social amoeba *Dictyostelium* to form a multicellular structure, sentinel cells are deployed to combat pathogens (*1*).

Generally, infection follows the entry of a bacterium into a host cell, giving rise to a pathogen-containing vacuole usually called a phagosome. From this common starting point, pathogens subvert or resist the mechanisms that usually transform the phagosome into a bactericidal environment. Understanding of the passive or triggered uptake mechanisms and of the subsequent hijacking of host cell processes is increasing steadily, but little is known about how the pathogens exit their primary host cells and spread the infection.

Mycobacterium tuberculosis causes tuberculosis and other granulomatous lesions and is a major threat to human health. *M. marinum* is a close relative (*3*) responsible for fish and amphibian tuberculosis, in which it causes almost indistinguishable pathologies and lesions [reviewed in (*4*)]. Several elegant cross-species complementation studies between these two pathogens highlight their common mechanisms of pathogenicity [reviewed in (*4*)].

After passive uptake by immune phagocytes, *M. tuberculosis* and *M. marinum* arrest or bypass phago-lysosome maturation and replicate inside a compartment of endosomal nature (*5*–*7*).

[1]Département de Biochimie, Faculté des Sciences, Université de Genève, Sciences II, 30 quai Ernest Ansermet, CH-1211 Genève-4, Switzerland. [2]Department of Microbiology and Immunology, College of Veterinary Medicine, Cornell University, Ithaca, NY 14853, USA.

*To whom correspondence should be addressed. E-mail: thierry.soldati@unige.ch

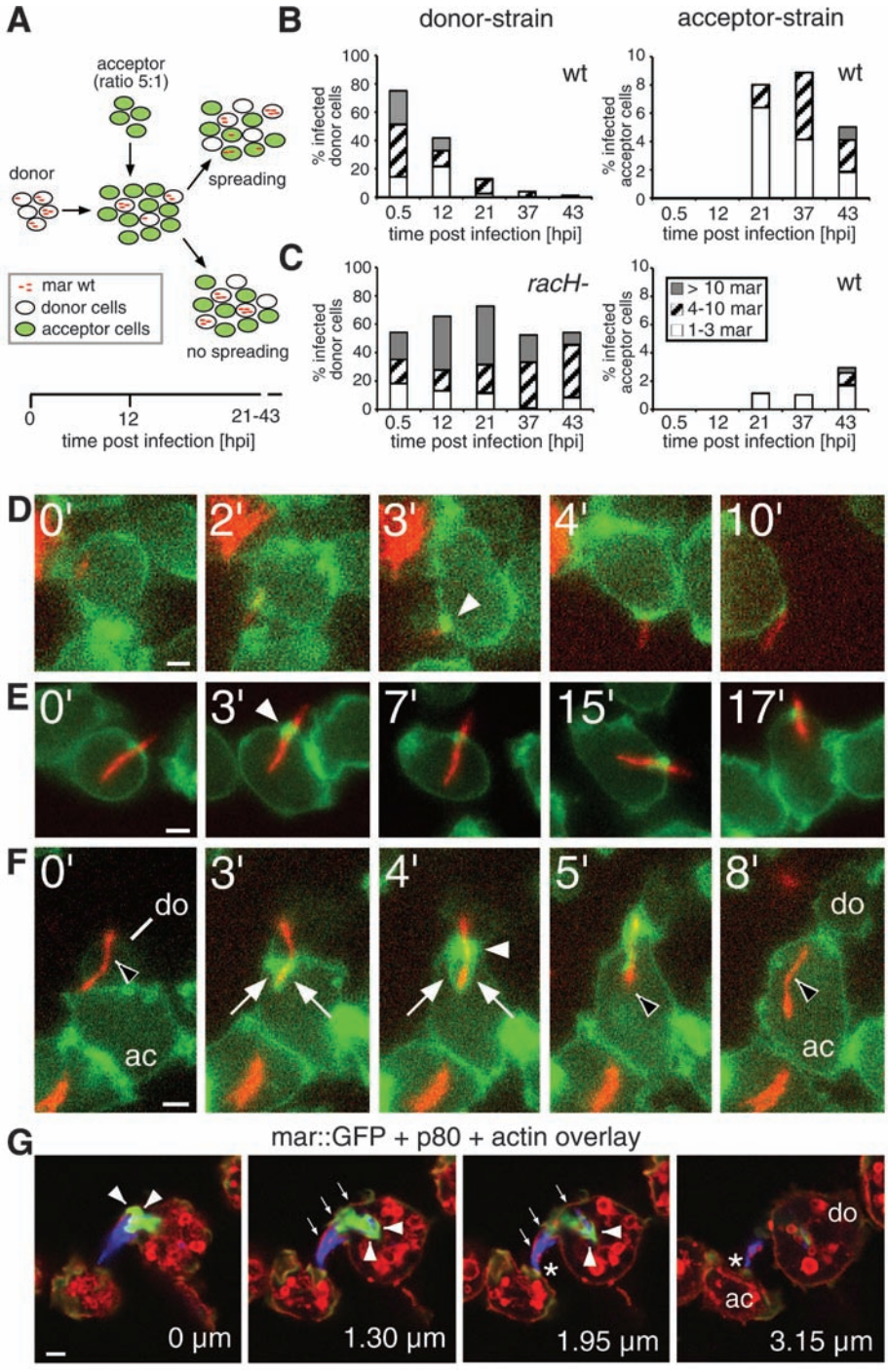

Fig. 1. Direct cell-to-cell transmission of *M. marinum* occurs via ejectosomes and is RacH-dependent. (**A**) Quantitative dissemination assay. A donor strain [wild-type (wt) or *racH*$^{-}$ cells] was infected with DsRed-expressing *M. marinum* (mar) and, at 12 hpi, mixed with a green fluorescent acceptor strain. The presence of bacteria in donor and acceptor cells was scored. Dissemination efficiency for wild-type (**B**) and *racH*$^{-}$ (**C**) donor cells is shown. The number of bacteria per cell (classified into groups of 1 to 3, 4 to 10, and >10 bacteria per cell) is indicated. [(D) to (F)] Live GFP–actin-binding domain (ABD)–expressing *Dictyostelium* cells (green) infected with DsRed-expressing *M. marinum* (red) were imaged at 35 hpi for the indicated times (upper left corners). (**D**) Nonlytic ejection of mycobacteria occurs through actin-dense ejectosomes (white arrowhead). (**E**) Cells with mycobacteria spanning the plasma membrane retain normal motility. (**F**) Cell-to-cell transmission of a cytosolic bacterium (black arrowhead) from a donor cell (do) to an acceptor cell (ac) through an ejectosome (white arrowhead) into a phagocytic cup (white arrows). (**G**) A bundle of bacteria is ejected from a donor cell (do). The plasma membrane bulge (small arrows) is ruptured at the tip (asterisk), where it contacts an acceptor cell (ac). Actin tails stained by phalloidin (green, arrowheads) were polarized at the posterior of bacteria (blue). The vertical distance from the first section is indicated in micrometers. Scale bars, 1 µm.

Both species can escape from this vacuole into the host cytosol (*8*–*11*), although at varying frequencies. Efficient translocation into the cytosol depends on an intact region of difference (RD) 1 locus (*10*, *11*), which encodes components of a type seven secretion system and essential secreted effectors (*12*). This ESX-1 secretion system has been implicated in the arrest of phagosome maturation (*13*), granuloma formation, and the spread of infection (*14*, *15*); however, it is not essential for replication inside macrophages (*14*). It has also been directly associated with the secretion of a membranolytic activity (*15*). Specifically, the secreted effector ESAT-6 has recently been linked to niche breakage and pore-forming activity in macrophages (*11*).

M. marinum and *M. tuberculosis* can disseminate through the release of bacilli after host cell lysis via necrotic or apoptotic cell death (*16*–*18*), but studies also document cell-to-cell, antibiotic-insensitive spreading inside an epithelial monolayer (*19*, *20*). *M. marinum* induces plasma membrane protrusions (*2*, *9*) suggested to participate in dissemination between macrophages in culture (*21*) and inside zebrafish embryos (*22*). Hence, escape into the cytosol may be a necessary precursor for cell-to-cell spread and may involve a direct nonlytic transmission process occurring within the granuloma (*5*, *6*).

We adopted the genetically tractable *Dictyostelium*–*M. marinum* model system to unravel basic mechanisms of intercellular dissemination. The course of *M. marinum* infection in *Dictyostelium* amoebas is very similar to that in macrophages (*8*). The mycobacteria replication vacuole accumulates a flotillin-like raft protein, then ruptures and releases *M. marinum* into the cytosol (fig. S1). A *Dictyostelium* mutant lacking the RacH guanosine triphosphatase (GTPase), which is involved in regulation of the actin cytoskeleton and endosomal membrane trafficking and acidification, was more permissive for *M. marinum* proliferation (*8*). Detailed fluorescence-activated cell sorting (FACS) analysis (fig. S2) of these infected cells suggested an interference with intercellular dissemination (fig. S3).

To test this hypothesis, we designed a quantitative dissemination assay (Fig. 1A). Briefly, an infected *Dictyostelium* donor strain (either wild-type or *racH*$^{-}$) was mixed with a green fluorescent wild-type acceptor strain at a donor:acceptor ratio of 1:5. Over the course of infection, the number of bacteria per donor cell and acceptor cell was determined by visual inspection. The proportion of wild-type infected donor cells decreased concomitantly with a sharp increase in infected acceptor cells at 21 hours post infection (hpi), and the number of bacteria per acceptor cell increased over time (Fig. 1B). This indicated successful transmission of bacteria and replication in acceptor cells. In contrast, the proportion of infected *racH*$^{-}$ donor cells remained relatively constant (above 50%). The infection of acceptor cells from *racH*$^{-}$ donor cells was about eight times less than from wild-type donor cells (Fig. 1C). The *racH*$^{-}$

cells were deficient in intercellular spreading of mycobacteria, and it appears that a RacH-dependent release mechanism is required for cell-to-cell transmission under these conditions.

Cytosolic pathogens such as *Listeria* and *Shigella* use actin-based tails and filopodia for intercellular spreading. During *M. marinum* infection of macrophages, unidentified mycobacterial proteins induce actin tails in a Wiskott-Aldrich syndrome protein–dependent manner (*23*), as well as structures reminiscent of *Shigella*-induced filopodia (*9*) that can be captured by neighboring cells (*9*) (fig S4). Hence, we monitored F-actin dynamics in infected cells expressing a green fluorescent protein (GFP) fusion with the actin-binding domain (ABD) of filamin (*24*) by live microscopy (movies S1 to S7; Fig. 1, D to F; and fig. S5, A and B). At late stages of infection, despite the presence of many cytosolic bacteria, cells exhibited apparently normal amoeboid motility (movie S1) and cell division (movie S2). In contrast to the observation in macrophages (*9*) (fig. S4), no persistent actin tails were visible on cytosolic bacteria, possibly due to the high rate of actin depolymerization in *Dictyostelium* (*25*). However, transient actin flashes were produced when bacteria contacted the cell cortex (fig. S5A and movie S3).

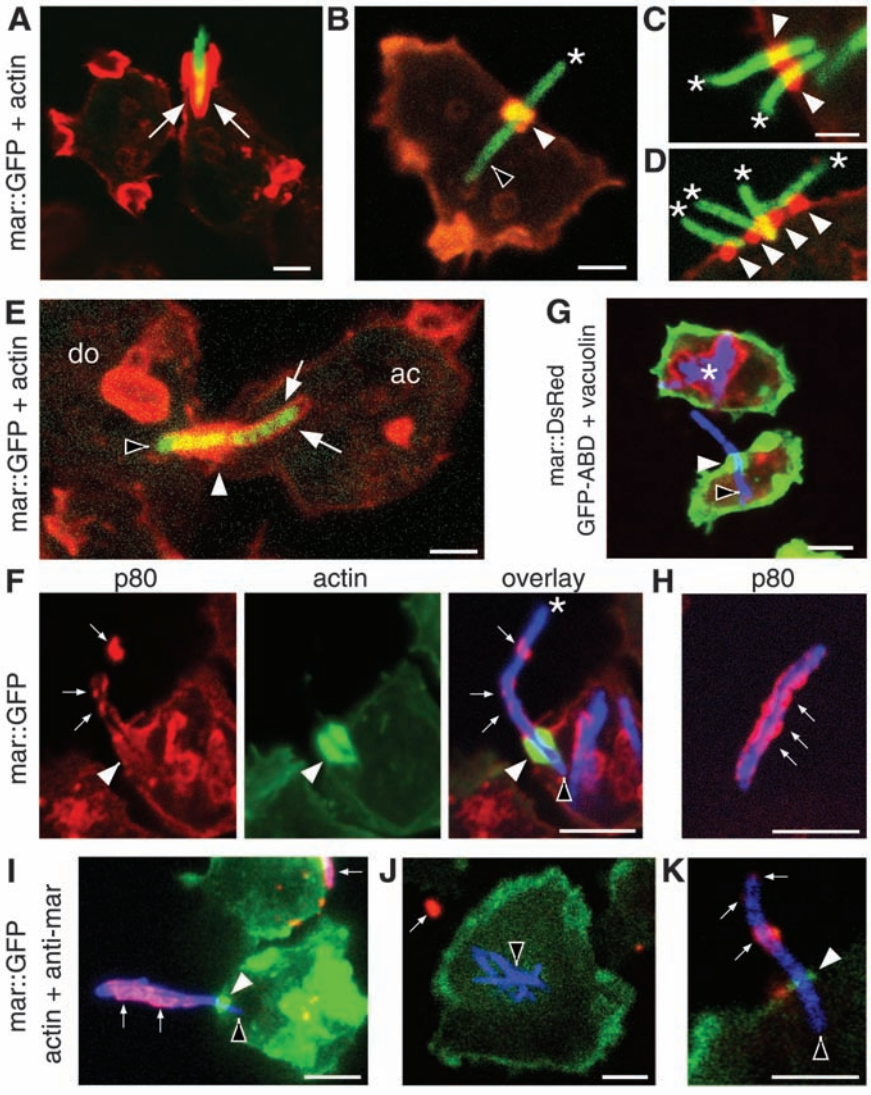

Fig. 2. Biogenesis, structure, and topology of ejectosomes. Paraformaldehyde-fixed cells infected with GFP-expressing *M. marinum* (green), stained for F-actin (red), are shown. (**A**) A phagocytic cup lined with F-actin (arrows). A single bacterium (**B**) or multiple bacteria (**C** and **D**) spanning the host cell plasma membrane (asterisks) through ejectosomes (white arrowheads), with the intracellular part of the bacterium devoid of actin labeling [black arrowhead in (B)]. (**E**) Cell-to-cell transmission of bacteria from a donor (do) to an acceptor (ac) cell through an ejectosome into a phagocytic cup (arrows). (**F**) The movement of cytosolic bacteria (blue) through ejectosomes (F-actin, green) induces a plasma membrane bulge (small arrows) that ruptures at the tip (asterisk). The intracellular part of the ejecting bacterium is devoid of p80, a plasma membrane marker (F), and vacuolin, a niche marker (asterisk in **G**). Some extracellular bacteria were positive for p80 (small arrows in **H**). (**I** to **K**) Live infected cells (*M. marinum*, blue; actin, green) were incubated in the presence of an anti–*M. marinum* serum. The extracellular parts of ejecting [small arrows in (I) and (K)] or outside [small arrow in (J)] bacteria were accessible to the antiserum and labeled red, in contrast to intracellular bacteria [black arrowhead in (J)], confirming partial loss of plasma membrane integrity. Scale bars, 1 μm.

Bacteria were ejected through an F-actin–dense structure we called an ejectosome (Fig. 1D and movie S4). Mycobacteria were also seen spanning the plasma membrane without inducing host cell lysis, a situation stable for the duration of the observation (17 min, Fig. 1E and movie S5). A substantial proportion of cells harbored multiple similar structures (fig. S5B and movie S6). Ejectosomes can apparently exert a contractile force, forming a tight septum around the bacteria as they are towed behind motile host cells (Fig. 1D and movie S4). We also captured images of synchronized ejection from a donor cell and phagocytosis by an acceptor cell (Fig. 1F and movie S7). Hence, an actin-based mechanism appeared to be responsible for non-lytic ejection of cytosolic mycobacteria, which, concomitantly with capture by neighboring cells, ensured efficient and antibiotic-insensitive intercellular spreading.

The live observations were confirmed by staining fixed infected cells with fluorescent phalloidin. During phagocytosis, the cell deforms toward the bacteria and extends lamellipodia that surround it along most of its length (Figs. 2A and 3E). In contrast, ejectosomes are short barrel-shaped structures usually found in flat membrane regions (Fig. 2B). Multiple ejectosomes were often observed to cluster at the surface of a cell (Fig. 2, C and D). Cell fixation preserved the structure of ejectosomes coupled to phagocytic cups, suggesting direct donor-to-acceptor transmission (Fig. 2E).

What propels bacteria during ejection is unclear, because we rarely observed bacteria with typical F-actin tails (Fig. 1G). Ejection may be powered by a mechanical process resulting from a combination of cortical tension, cytoplasmic pressure, and a reaction of the actin cortex to bacteria-induced deformation. The ejectosome was strongly enriched in myosin IB and coronin (fig. S5, G and H), whereas the F-actin barrel was weakly or not at all enriched in myosin II and the Arp2/3 complex (fig. S5, I and J). Thus, the ejectosome may either assemble de novo or result from a rearrangement of preexisting cortical structures.

In all cases of ejection, the part of the bacterium inside the cell was devoid of membrane markers from endosomes (Fig. 2F and fig. S5C) or the replication compartment (Fig. 2, F and G), which means that the phenomenon is not an exocytic event. The protruding part of the bacterium induced a bulge in the plasma membrane (Fig. 2F and fig. S5C), demonstrating that the bacterium is on an outward journey through the cell surface. The membrane labeling often appeared

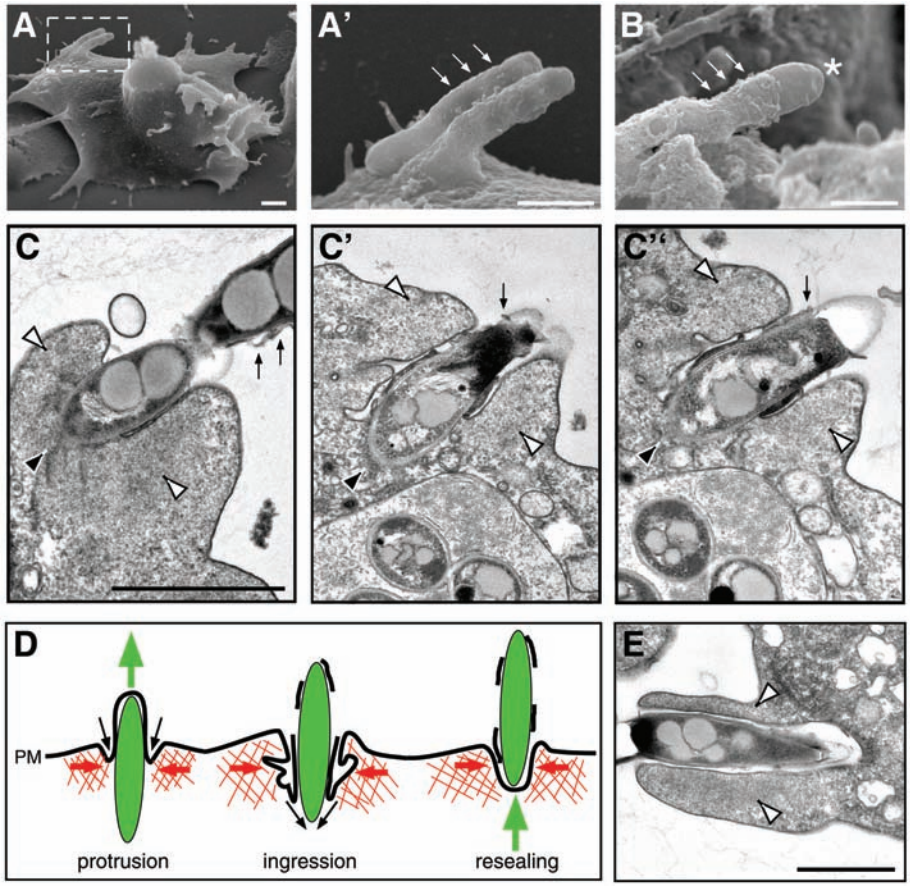

Fig. 3. Electron microscopy of ejecting bacteria and schematic representation of an ejection event. Scanning electron microscopy [**A** and **B**; **A'** is the magnified inset of (A)] showed bulges of the plasma membrane (small arrows), some ruptured at the tip of the ejecting bacterium [(B), asterisk]. Scale bars, 0.5 μm. (**C** to **C''**) Serial sections through an ejectosome revealed the organization of the F-actin (white arrowheads) and the plasma membrane. The posterior of the ejecting bacterium (black arrowhead) was in the cytosol. The bacterium was separated from the F-actin by the invaginated plasma membrane, which was tightly apposed to its surface. Membrane fragments were scattered along the extracellular part of the bacterium (small arrows). (**D**) Schematic representation of an ejection. During outward movement of a bacterium (green), the F-actin barrel exerts contraction (red arrows), and the invaginating plasma membrane (PM) reseals at the posterior of the bacterium (black arrows), maintaining a tight septum despite partial membrane rupture. (**E**) Micrograph of a phagocytic cup. The actin-filled lamellipodia (white arrowheads) extend and engulf a bacterium. Scale bars, 1 μm.

patchy at the tip of the bulge (Fig. 2F and fig. S5C), suggesting local loss of integrity. Sometimes, extracellular mycobacteria were wrapped in plasma membrane remnants (Fig. 2H and fig. S5D). Outward plasma membrane deformation (Fig. 3, A and C) and partial membrane rupture (Fig. 3, B and C) were also observed by scanning and transmission electron microscopy.

Labeling of the protruding part of ejected *M. marinum* with an anti–*M. marinum* serum in nonpermeabilized cells indicated the accessibility of the bacterium surface and hence local loss of plasma membrane integrity (Fig. 2, I and K). However, infected cells do not lyse, as judged by live imaging (Fig. 1E and movies S1 to S7), and they are also not leaky, as demonstrated by the exclusion of a membrane-impermeant DNA-binding dye during a 2-hour-long incubation (fig. S5E). Serial sections through an ejectosome (Fig. 3C) showed a cytosolic bacterium protruding from a cell, with the plasma membrane ruptured toward the tip of the bacterium but at the same time invaginated between the bacterium and a zone of dense actin meshwork. We propose that, during ejection, the ingressing plasma membrane stays tightly apposed to the bacterium surface and finally reseals at the posterior of the bacterium, resulting in a dynamic but tight seal that prevents host cell lysis or leakage (schematically depicted in Fig. 3D).

During *Dictyostelium* infections, *M. tuberculosis* was first found in spacious vacuoles (fig. S7) that accumulated vacuolin, the *Dictyostelium* flotillin homolog (fig. S6A). Then, with an efficiency lower than that of *M. marinum*, the bacilli translocated into the cytosol (Fig. 4A and figs. S6A and S7), where they induced ejectosomes (Fig. 4A and fig. S6, B and C). In *Dictyostelium*, *M. avium* also accumulated in spacious compartments decorated with vacuolin, but, in contrast to *M. tuberculosis* and *M. marinum*, no vacuole breakage was detected (Fig. 4A) and no ejectosome was observed. Vacuole escape and nonlytic ejection from the host cell may be conserved strategies among tubercular mycobacteria that could play a prominent role in the dissemination of infection, rather than intracellular survival per se.

We expected a direct correlation between the observed number of ejectosomes and the spreading of infection. Indeed, in wild-type cells, there were about 15 ejectosomes per 100 cells at 37 hpi, whereas no ejectosome was ever observed in *racH*$^{-}$ cells (Fig. 4B and fig. S8B). This is not due to deficient vacuole escape, because at 37 hpi, over 90% of *M. marinum* were cytosolic and free of vacuolin staining, as compared to 75% in wild-type cells (Fig. 4B and fig. S9). Complementation of *racH*$^{-}$ cells with GFP-RacH partially restored the capacity to form ejectosomes (fig. S8C). In accordance with this observation, membrane fragments carrying GFP-RacH polymerize actin around them upon the addition of guanosine 5′-*O*-(3′-thiotriphosphate) in a cell-free assay (*26*).

In correlation with the capacity to induce ejectosomes, the RD1 locus is present in *M. tuberculosis* and *M. marinum* (*13*–*15*) but absent from *M. avium* (*12*). A *M. marinum* mutant deleted of its RD1 locus (ΔRD1) replicated inefficiently in *Dictyostelium* (Fig. 4D), and the population of infected cells steadily decreased with time (Fig. 4E and fig. S8D). Vacuole escape was readily detectable (Fig. 4B and fig. S9) but was about four to five times less efficient than for wild-type *M. marinum*, as measured by colocalization with vacuolin or p80. This corroborates recent findings in macrophages when a collection of ESX-1 mutants was used (*11*). But the most striking observation was the complete absence of ejectosomes (Fig. 4B). If the ESX-1 locus secretes vacuole escape factors (*11*), it may also secrete factors that coordinate the egress of the resulting cytosolic bacteria. It is possible that ESAT-6, one of the major secreted effectors, plays a role in both processes. We designed a trans-complementation strategy in which *M. marinum* ESAT-6 was conditionally expressed directly inside the cytosol of *Dictyostelium* (Fig. 4C). *M. marinum* ΔRD1 apparently replicated better in ESAT-6–expressing cells than in wild-type cells (Fig. 4D) and showed a 1.5- to 2-fold increased frequency of niche escape. Most important, it induced ejectosome formation (Fig. 4B). Our data demonstrated that the nonlytic ejection of tubercular mycobacteria from *Dictyostelium* is a concerted process

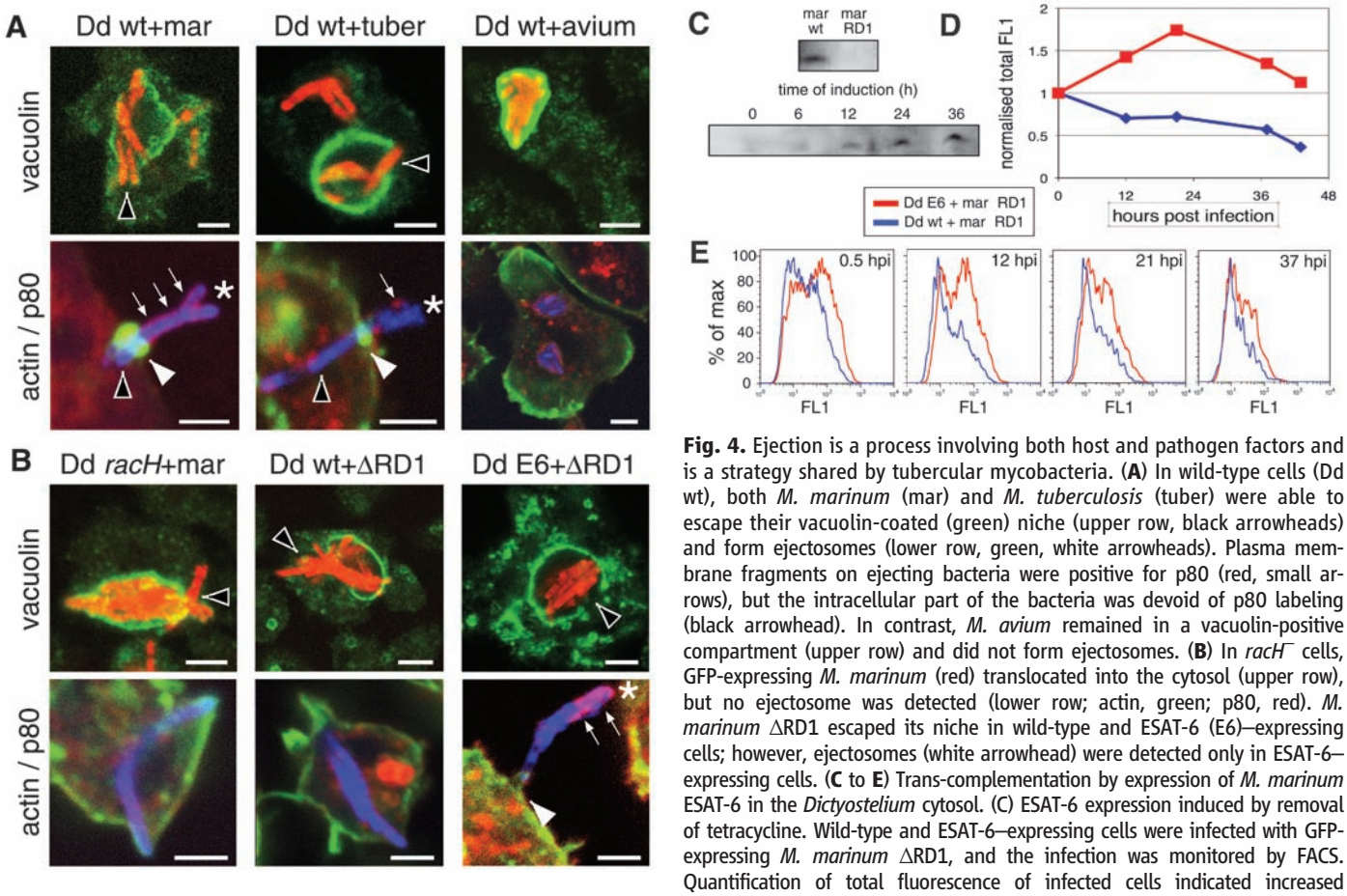

Fig. 4. Ejection is a process involving both host and pathogen factors and is a strategy shared by tubercular mycobacteria. (**A**) In wild-type cells (Dd wt), both *M. marinum* (mar) and *M. tuberculosis* (tuber) were able to escape their vacuolin-coated (green) niche (upper row, black arrowheads) and form ejectosomes (lower row, green, white arrowheads). Plasma membrane fragments on ejecting bacteria were positive for p80 (red, small arrows), but the intracellular part of the bacteria was devoid of p80 labeling (black arrowhead). In contrast, *M. avium* remained in a vacuolin-positive compartment (upper row) and did not form ejectosomes. (**B**) In *racH*$^{-}$ cells, GFP-expressing *M. marinum* (red) translocated into the cytosol (upper row), but no ejectosome was detected (lower row; actin, green; p80, red). *M. marinum* ΔRD1 escaped its niche in wild-type and ESAT-6 (E6)–expressing cells; however, ejectosomes (white arrowhead) were detected only in ESAT-6–expressing cells. (**C** to **E**) Trans-complementation by expression of *M. marinum* ESAT-6 in the *Dictyostelium* cytosol. (C) ESAT-6 expression induced by removal of tetracycline. Wild-type and ESAT-6–expressing cells were infected with GFP-expressing *M. marinum* ΔRD1, and the infection was monitored by FACS. Quantification of total fluorescence of infected cells indicated increased replication of *M. marinum* ΔRD1 in ESAT-6 expressers [(D), red curve, normalized to the total fluorescence values at time 0.5 hpi]. Infected ESAT-6 expressers with high fluorescence (FL1) persisted longer [(E), red curve] than did infected wild-type *Dictyostelium* [(D) and (E), blue curve].

that necessitates host and pathogen factor(s) and is crucial for the maintenance of an infection in a cell population.

Conceptually, the ejectosome bears intriguing analogies with the contracting actin ring formed during purse-string closure of membrane wounds in *Xenopus* oocytes (*27*) and during the repair of toxin-induced macroapertures in endothelial cells (*28*). Because lytic release from a single-celled amoeba would be lethal, the ejectosome may have first evolved as a plasma membrane repair mechanism. This concerted and mutually beneficial strategy might have been conserved during evolution to ensure the dissemination of mycobacteria between the immune phagocytes of their metazoan host.

Dictyostelium can be thought of as a rudimentary innate immune phagocyte, and this model has allowed us to identify a conserved strategy for egress and cell-to-cell spread that is shared by *M. marinum* and *M. tuberculosis*.

References and Notes

1. G. Chen, O. Zhuchenko, A. Kuspa, *Science* **317**, 678 (2007).
2. L. M. Stamm, E. J. Brown, *Microbes Infect.* **6**, 1418 (2004).
3. T. P. Stinear *et al.*, *Genome Res.* **18**, 729 (2008).
4. D. M. Tobin, L. Ramakrishnan, *Cell. Microbiol.* **10**, 1027 (2008).
5. D. G. Russell, *Nat. Rev. Microbiol.* **5**, 39 (2007).
6. C. L. Cosma, D. R. Sherman, L. Ramakrishnan, *Annu. Rev. Microbiol.* **57**, 641 (2003).
7. K. H. Rohde, R. B. Abramovitch, D. G. Russell, *Cell Host Microbe* **2**, 352 (2007).
8. M. Hagedorn, T. Soldati, *Cell. Microbiol.* **9**, 2716 (2007).
9. L. M. Stamm *et al.*, *J. Exp. Med.* **198**, 1361 (2003).
10. N. van der Wel *et al.*, *Cell* **129**, 1287 (2007).
11. J. Smith *et al.*, *Infect. Immun.* **12**, 5478 (2008).
12. A. M. Abdallah *et al.*, *Nat. Rev. Microbiol.* **5**, 883 (2007).
13. T. Tan, W. L. Lee, D. C. Alexander, S. Grinstein, J. Liu, *Cell. Microbiol.* **8**, 1417 (2006).
14. H. E. Volkman *et al.*, *PLoS Biol.* **2**, e367 (2004).
15. L. Y. Gao *et al.*, *Mol. Microbiol.* **53**, 1677 (2004).
16. S. C. Derrick, S. L. Morris, *Cell. Microbiol.* **9**, 1547 (2007).
17. M. Chen, H. Gan, H. G. Remold, *J. Immunol.* **176**, 3707 (2006).
18. J. M. Davis, L. Ramakrishnan, *Cell* **136**, 37 (2009).
19. T. F. Byrd, G. M. Green, S. E. Fowlston, C. R. Lyons, *Infect. Immun.* **66**, 5132 (1998).
20. J. Castro-Garza, C. H. King, W. E. Swords, F. D. Quinn, *FEMS Microbiol. Lett.* **212**, 145 (2002).
21. F. Carlsson, E. J. Brown, *J. Cell. Physiol.* **209**, 288 (2006).
22. J. M. Davis *et al.*, *Immunity* **17**, 693 (2002).
23. L. M. Stamm *et al.*, *Proc. Natl. Acad. Sci. U.S.A.* **102**, 14837 (2005).
24. E. Lee, D. A. Knecht, *Traffic* **3**, 186 (2002).
25. S. H. Zigmond, *Cell Motil. Cytoskeleton* **25**, 309 (1993).
26. B. P. Somesh, C. Neffgen, M. Iijima, P. Devreotes, F. Rivero, *Traffic* **7**, 1194 (2006).
27. C. A. Mandato, W. M. Bement, *J. Cell Biol.* **154**, 785 (2001).
28. L. Boyer *et al.*, *J. Cell Biol.* **173**, 809 (2006).

29. We gratefully acknowledge L. Ramakrishnan and C. Cosma for providing strains of *M. marinum,* various GFP expression vectors, and advice; G. Griffiths for GFP-expressing *M. avium*; B. C. VanderVen for providing GFP-expressing *M. tuberculosis*; F. Rivero and M. Maniak for providing *Dictyostelium* mutant strains; C. Bauer of the National Center of Competence in Research imaging platform for his help with microscopy; P. Walther and E. Schmid for their expert help with the SEM; and D. Soldati for critical reading of the manuscript. The work was supported by the Swiss National Science Foundation in the form of a grant to T.S. and an individual short-term fellowship to M.H. The T.S. group participates in the NEMO (nonmammalian experimental models for the study of bacterial infections) network supported by the Swiss 3R Foundation. D.G.R. and K.H.R. are supported by grants AI 067027 and HL 055936 from the U.S. NIH.

Supporting Online Material

www.sciencemag.org/cgi/content/full/323/5922/1729/DC1
Materials and Methods
Figs. S1 to S9
References
Movies S1 to S7

5 December 2008; accepted 6 February 2009
10.1126/science.1169381